

## Chapter 1

# STATISTICAL APPROACH TO PHOTON LOCALIZATION

A. Z. Genack and A. A. Chabanov

*Department of Physics, Queens College*

*City University of New York*

*Flushing, New York 11367, USA*

genack@qc.edu

**Abstract** A statistical description of wave propagation in random media is necessary to characterize large fluctuations found in these samples. The nature of fluctuations is determined by the closeness to the localization transition. In the absence of inelastic processes, this can be specified, in many circumstances, by a single parameter - the ensemble average of the dimensionless conductance. As a result, the extent of localization can be determined by any of a wide variety of related statistical measurements. Among the quantities that most directly reflect key aspects of localization are the following: (i) the ensemble average of the dimensionless conductance, (ii) the degree of spatial correlation of intensity, (iii) the variances of the probability distribution of transmission quantities, such as the intensity, the total transmission, and the dimensionless conductance, and (iv) the ratio of the width to the spacing of modes of an open sample. We will emphasize the relationships between key statistical aspects of propagation in quasi-one-dimensional samples and the different impact of absorption upon these.

We find that even in the presence of absorption, the extent of localization can be characterized by a single parameter - the variance of the total transmission normalized by its ensemble average. Measurements of fluctuations in intensity and total transmission of microwave radiation allow us to study photon localization in collections of dielectric spheres and in periodic metallic wire meshes containing metallic scatterers. We find in low-density collections of alumina spheres contained in a copper tube, at frequencies near the first Mie resonance, that the variance of normalized total transmission scales exponentially once it becomes greater than unity. When this parameter is large, transmission spectra are observed to be a series of narrow lines with widths that are smaller than the separation between peaks. These spectra have an extraordinarily wide intensity distribution and correspondingly large variance. These results demonstrate that

the variance of normalized transmission serves as a powerful guide in the search for and characterization of photon localization.

**Keywords:** statistics, photon localization, microwave

## 1. INTRODUCTION

Waves are the means by which we probe our environment and communicate with one another. Their study has expanded from primordial fascination with everyday observations of ripples in a pond and the ocean's waves to the systematic study of sound, light and the full gamut of electromagnetic radiation, and quantum mechanical waves. The field of electromagnetic propagation has grown with the development of the laser to encompass the exploration of non-linear and quantum optical phenomena in an expanding array of new materials including optical fibers and photonic band gap structures. The joint application of optics and electronics in communications has made photonics a rapidly expanding aspect of modern life. The study of transport in random media has grown apace. It has been spurred in recent years by advances in imaging, by the interchange with electronic mesoscopic physics, and by the expanding range of statistical aspects of propagation that can be measured and computed.

Wave transport in random media is essentially a statistical problem [1, 2, 3, 4, 5]. Since the precise structure of a random sample is not known, the fine-grained variation in intensity of reflected and transmitted light cannot be predicted. An example of a random intensity pattern produced in reflection of a helium-neon laser beam from a sheet of paper is shown in Fig. 1.1. Similar speckle patterns

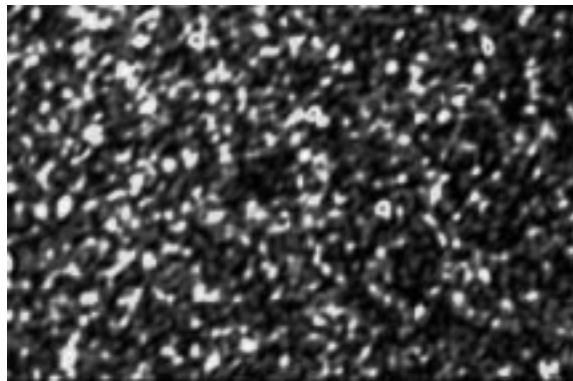


*Figure 1.1* The far-field speckle pattern of reflected light is seen in this CCD image of a helium-neon laser beam scattered from a sheet of white paper. Lighter regions have higher intensity.

are produced in transmission. Despite the apparently haphazard character of

scattered light, the nature of transport in a random medium can be obtained from a statistical characterization of such complex random speckle patterns for all incident frequencies and incident spatial modes for an ensemble of statistically equivalent random realizations. An example of a spectral "speckle" pattern of microwave intensity at a point on the output surface of a random sample is shown in Fig. 1.2. The sample is composed of polystyrene spheres randomly

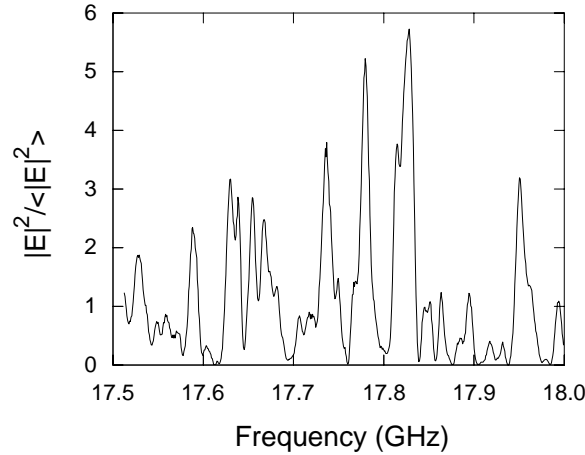


*Figure 1.2* Normalized spectrum of the intensity of a single polarization component of the microwave field transmitted through a random collection of 1.27-cm-diam. polystyrene spheres contained in a 100-cm-long waveguide. Only a single polarization component is detected using a wire antenna positioned at the sample output surface. Its amplitude is squared and divided by the ensemble average of this quantity.

positioned in a long copper tube. An even more detailed "fingerprint" of the sample is contained in the spatial and spectral variation of the field itself.

The field is the sum of randomly phased partial waves associated with all possible paths from the source to the point of detection. The field fluctuates with position because of the changing set of partial waves that contribute to the field at different points. The linear superposition of such partial waves corresponds to the sum of phasors shown schematically in Fig. 1.3. Each partial wave may be represented by an arrow or phasor with length proportional to the field amplitude and with phase equal to that of the partial wave. The component of the phasor along the x-axis (y-axis) gives the component of the field, which is in-phase (out-of-phase) with the incident wave. The fluctuations in the field with frequency shift at a given point are primarily due to changes in the phase difference,  $\Delta\varphi = 2\pi\Delta s/\lambda$ , between partial waves, which differ in

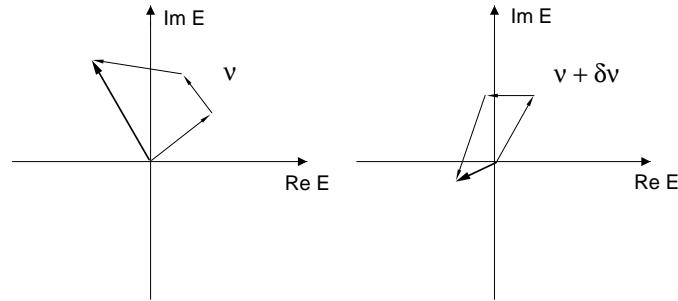


*Figure 1.3* Partial waves associated with different trajectories are shown as phasors and summed to give the total field. Each phasor is a complex-valued contribution  $E$  with real part corresponding to the in-phase component and imaginary part corresponding to the out-of-phase component of the partial wave.

path length by  $\Delta s$ , as a result of the change in wavelength  $\lambda$ . Measurements of the microwave field at the same point and in the same sample configuration as in Fig. 1.2 are shown in Fig. 1.4a. Both the in- and out-of-phase components of the transmitted field are measured. The intensity in Fig. 1.2 is calculated as the sum of the squares of the in- and out-of-phase components. The magnitude of the field  $|E|$  and the phase modulus  $2\pi, \phi$ , are computed from these components and the resultant spectra are displayed in Fig. 1.4b.

In order to describe the nature of transmission in a random medium, the full probability distributions of random variables should be given rather than their ensemble averages. These distributions reflect correlation within the medium, whose dependence upon position and frequency give key static and dynamic aspects of average transmission. Let us consider, for example, correlation functions of the field. The field correlation function with displacement on the sample surface for an ensemble of samples is the Fourier transform of the variation of the ensemble average of the far-field intensity with angle [6]. Similarly, the field correlation function with frequency shift is the Fourier transform of the time-of-flight distribution of radiation reaching a point [7, 8]. Thus considerable insight is gained by dealing with field correlation functions, which involve both the amplitude and phase of the wave.

It is often convenient, however, to consider these variables separately [9]. Key aspects of the statistics of steady-state transmission with monochromatic sources can be obtained from measurements of distribution [1, 2, 10, 11, 13, 14, 15, 16, 21, 22, 23, 26, 28, 29, 32, 33, 34, 35, 36, 37, 38, 39, 41, 42, 43, 44, 45] and correlation [15, 17, 18, 19, 20, 22, 23, 24, 25, 27, 30, 31, 42, 43, 45]

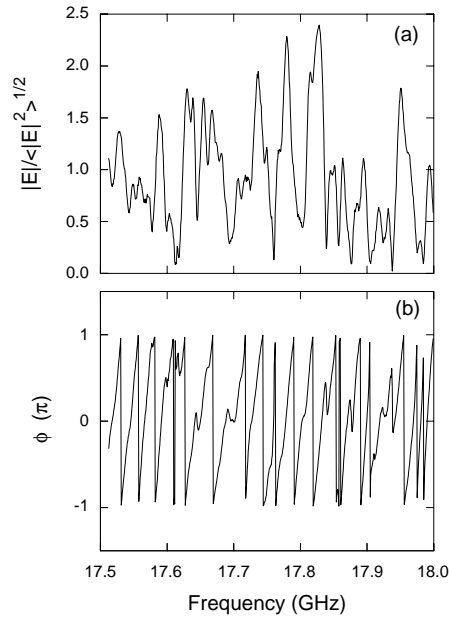


Figure 1.4a The real and imaginary parts of the microwave field at the same point and in the same sample configuration as in Fig. 1.2.

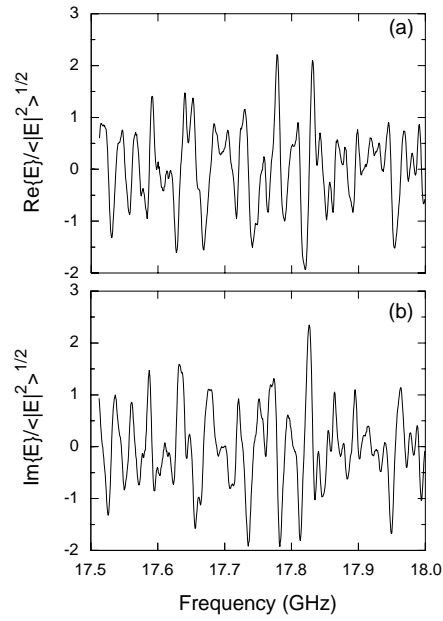


Figure 1.4b The magnitude  $|E|$  normalized to its ensemble average value and the phase, modulus  $2\pi$ ,  $\phi$ , of the microwave field calculated using the data in Fig. 1.4a.

of the local intensity,  $|E|^2$ , or of the spatially averaged flux. At the same time, basic aspects of the statistics of dynamics are revealed by measuring the probability distribution of the frequency derivative of the cumulative phase  $\varphi$  [47, 48, 49, 50, 51, 9, 52, 53, 54]. The cumulative phase is obtained by incrementing  $\phi$  of Fig. 1.4b by  $2\pi$  each time the phase passes through the upper bound of  $\phi$  of  $\pi$  rad. The derivative  $d\varphi/d\omega$  equals the average photon transit time of a narrow band pulse from the source to the detector. Large fluctuations in steady-state and dynamic transmission quantities are a distinguishing feature of transport in random media. Here we will focus on the statistics of static transmission quantities.

The study of statistics provides a platform for the characterization of the localization transition. Though initially proposed in the electronic context [55, 56, 57], the Anderson transition has been a model for the study of classical waves in random media [3, 5]. Because of the powerful experimental methods available for studying classical waves, a rich statistical portrait can be obtained, which illuminates electronic transport. Measurements of the distribution and

correlation of local transmission quantities and of dynamics in random ensembles, for example, have not been carried out in electronic samples. It is also of particular interest to investigate the Anderson transition for classical waves because the complication of electron-electron interactions is absent. Finally, new aspects of transport and novel applications of propagation and localization result from the study of electromagnetic radiation because of the possibilities of spontaneous and stimulated emission and absorption of photons.

## 2. FLUCTUATIONS IN STEADY-STATE TRANSMISSION

Making the assumption that the scattered field can be represented as a superposition of a large number of statistically independent partial waves, the probability distribution of the in- and out-of-phase components of the amplitude of polarized monochromatic radiation is a Gaussian [37], while the distribution of  $\varphi$  is a Gaussian [9] and the distribution of  $\phi$  is flat [2]. The corresponding intensity distribution was calculated by Rayleigh [10] and bears his name. For a given polarization component of the field, the probability distribution of the associated intensity is a negative exponential. When the intensity is normalized to its average value for an ensemble of equivalent samples, its distribution is a universal function independent of the physical dimensions or scattering strength of the sample,  $P(s_{ab} = T_{ab}/\langle T_{ab} \rangle) = \exp(-s_{ab})$ . Here  $T_{ab}$  is the transmission coefficient from an incident mode  $a$  into an outgoing mode  $b$ , and  $\langle \dots \rangle$  represents the average of the quantity between the brackets over an ensemble of statistically equivalent samples. Depending upon the experiment under consideration, these modes may correspond to different transverse momentum states of the far field, or to different modes of a microwave cavity, or to the fields within different coherence areas on the sample surface. A schematic representation of key transmission quantities is presented in Fig. 1.5. For this

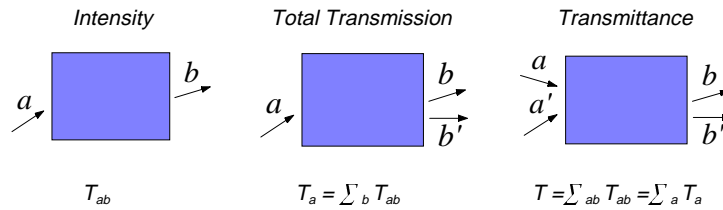


Figure 1.5 Transmission coefficients in random media in order of increasing spatial averaging. The incident and outgoing modes  $a$  and  $b$  may be in any complete representation of the field.

negative exponential distribution for a single polarization component of the

radiation,  $\text{var}(s_{ab}) = 1$ . Thus the variance of the intensity is equal to its average value. Since this exponential distribution is universal, a measurement of the distribution provides no information regarding wave propagation beyond the confirmation of the reasonableness of the model. However, the average transmission,  $\langle T_{ab} \rangle$ , which is the first moment of the transmission distribution, depends upon the absorption coefficient and scattering strength of the medium, and both the transport mean free path  $\ell$  and the diffusive absorption length  $L_a$  can be determined from the scaling of  $\langle T_{ab} \rangle$ . In particular, when absorption is absent,  $\langle T_{ab} \rangle \sim \ell/L$  [1, 7].

As a result of spatial correlation, however, waves are not statistically independent and deviations from the Rayleigh distribution are observed. Short-range intensity correlation is associated with field correlation and reflects the inability of a wave to change on a scale much shorter than the wavelength [15]. Its presence is immediately evident in the speckle pattern of laser radiation scattered from an object, such as that shown in Fig. 1.1. For an illuminated area  $A$  and wavelength  $\lambda$ , the number of transverse modes for a vector wave is equal to the number of speckle spots,  $N = 2\pi A/\lambda^2$ . Since the number of partial waves associated with distinct paths within the medium, which contribute to the field at a point, greatly exceeds  $N$ , these waves must be correlated and departures from Rayleigh statistics can be expected. In addition, scattering in the medium and subsequent diffusion induce intensity correlation across the entire sample. In quasi-one-dimensional samples, which have reflecting walls and length  $L$  much greater than the transverse dimensions of the sample, modes are completely mixed and there is consequently a constant component of intensity correlation between points in the transmitted wave [17, 20, 22, 24, 27]. The cumulant correlation function of normalized intensity is  $C = \langle \delta s_{ab} \delta s_{ab'} \rangle$ , where  $\delta s_{ab} = s_{ab} - 1$  is the fluctuation from the ensemble average value of  $s_{ab}$ . The degree of long-range correlation may be represented by  $\langle \delta s_{ab} \delta s_{ab'} \rangle$ , where  $b$  and  $b'$  are points separated by several intervening speckle spots. The actual variation with position on the output surface of the degree of intensity correlation for an ensemble of randomly positioned polystyrene spheres, such as those whose spectra are shown in Fig. 1.4a and 1.4b is presented as the filled circles in Fig. 1.6 [46]. The correlation function has a short-range oscillatory component in addition to a constant background. The main part of the oscillatory component arises from the correlation in the field. This component of the normalized intensity cumulant correlation function with displacement  $\Delta R$  is given by  $|\langle E(R)E(R + \Delta R) \rangle|^2 / (\langle |E(R)|^2 \rangle \langle |E(R + \Delta R)|^2 \rangle)$  and can be computed directly from measurements of the field. It is shown as the circles in Fig. 1.6. This field factorization contribution to the cumulant correlation function of normalized intensity,  $C$ , is denoted  $C_1$  and equals unity at  $\Delta R = 0$  [15, 17, 42]. The constant background contribution to  $C$  is dominated by a term denoted by  $C_2$ , which is calculated by including a single crossing of fields in

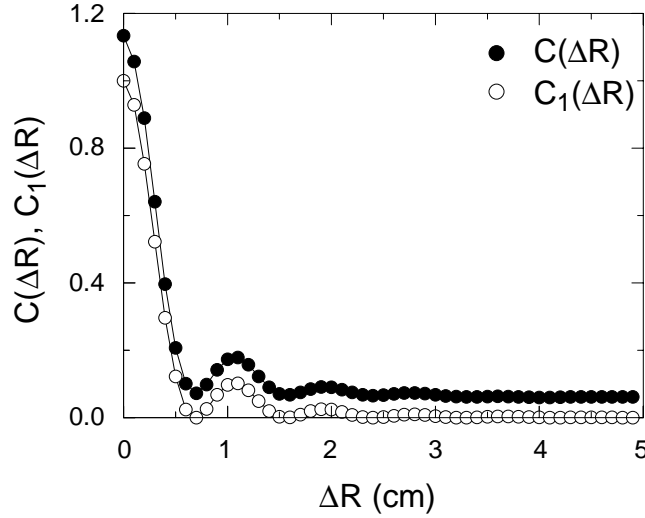


Figure 1.6 Normalized cumulant correlation functions with displacement of the intensity,  $C$ , and the square of the field correlation function,  $C_1$ , for the sample described in Fig. 1.2 and in the text. The difference between  $C$  and the short-range correlation function  $C_1$  is the contribution associated with long-range correlation.

the medium, represented by a Hikami box in a perturbation expansion of the Green function [17, 20]. In the absence of absorption or gain, the degree of long-range correlation is proportional to  $L/N\ell$  [17, 20, 22, 24, 27].

The impact of spatial correlation upon distributions of transmission quantities is perhaps most transparent for the distribution of the total transmission for a given incident mode  $a$ , normalized by its ensemble average value,  $P(s_a = T_a/\langle T_a \rangle)$ , where  $T_a = \sum_b T_{ab}$  is the sum of transmission coefficients over all output modes, as shown schematically in Fig. 1.5. If the intensity at different points were uncorrelated, transmission would be the sum of statistically independent fluxes at an unbounded number of points. The total transmission distribution would then be a delta function. However, as a result of short-range correlation in the intensity, there can be no more than  $N$  coherence areas in the transmission speckle pattern. Thus, if there were no correlation in the flux in distinct coherence areas, we would expect that the variance of the normalized total transmission resulting from the sum of  $N$  contributions, each of order  $1/N$ , would be  $N(1/N)^2 = 1/N$ . Instead, for diffusing waves in the absence of absorption, the variance is larger by a factor of  $L/\ell$ , giving  $\text{var}(s_a) \sim L/N\ell$ , which equals the degree of long-range correlation. Thus enhanced fluctuations

in transmission are the result of extended spatial correlation and the distribution of the normalized total transmission reflects the nature of scattering in the medium.

For quasi-one-dimensional samples, Kogan and Kaveh [34] found that the distribution  $P(s_{ab})$  can be expressed in terms of the distribution  $P(s_a)$ ,

$$P(s_{ab}) = \int_0^\infty \frac{ds_a}{s_a} P(s_a) \exp(-s_{ab}/s_a). \quad (1.1)$$

This relationship was found using random matrix theory. It has been confirmed in microwave measurements [41] in random polystyrene samples both with and without the influence of absorption, for diffusive waves and at the threshold of localization, as will be shown below. It is seen from Eq. (1.1), that negative exponential intensity statistics would only be obtained if the distribution of the total transmission were a delta function. But, since spatial correlation is always present to some degree, deviations from Rayleigh statistics are present as well. The intensity distribution displays the extent of this correlation and hence displays the nature of transport within the sample. Random matrix theory gives the relation between the moments of two distributions, [34]

$$\langle s_{ab}^n \rangle = n! \langle s_a^n \rangle. \quad (1.2)$$

Again, measurements establish that this relation holds independent of the degree of spatial correlation or of absorption of the wave [44].

The existence of intensity correlation at separations well beyond a field coherence length was first recognized in the analysis of fluctuations observed in the electrical conductance of micron-sized samples at low temperatures [12, 13, 14]. Such samples are intermediate in size between the atomic and macroscopic scales and so are termed mesoscopic. The electronic wave function is coherent on a time scale longer than the diffusion time within mesoscopic samples. Hence the field inside the sample is temporally coherent with the incident field. As a result of extended spatial correlation of the current transmission coefficients between any pairs of incident and outgoing modes, the size of conductance fluctuations in mesoscopic conducting samples is enhanced by a factor of  $(L/\ell)^2$  and is independent of the scattering strength and sample size [13, 14, 40]. Expressing the conductance as  $G = (e^2/h)g$ , where  $g$  is the dimensionless conductance, the variance of  $g$  for mesoscopic samples is 2/15. The Landauer relation [60] gives  $g$  as the sum of transmission coefficients connecting all incident and outgoing modes,  $g \equiv T = \sum_{ab} T_{ab}$ , as illustrated in Fig. 1.5. In the following, we will also use the notation  $g$  to denote its ensemble average.

This incoherent sum is appropriate for physical measurements of conductance, in which temporal averages are taken over times long compared to the phase coherence time of incident current modes. Expressing the dimensionless conductance  $g$ , or equivalently the transmittance  $T$ , in terms of the total transmission,  $T = \sum_a T_a$ , one obtains  $g = \langle T \rangle = N\ell/L$ , for diffusive

waves in the absence of absorption. Thus,  $\text{var}(s_a) = \langle \delta s_{ab} \delta s_{ab'} \rangle \sim 1/g$ , suggesting a relationship between fluctuations of total transmission, spatial correlation of intensity, and average transport. Universal conductance fluctuations for diffusive waves corresponds to  $\text{var}(g) \simeq 2/15$  or, equivalently,  $\text{var}(s = T/\langle T \rangle) \simeq 2/15g^2$ . This enhancement arises from the equal extent of correlation of transmission coefficients  $T_{ab}$  for all input and output modes associated with a term in perturbation theory which includes two Hikami boxes. The contribution to  $C$  of this term is proportional to  $1/g^2$  and is referred to as  $C_3$  or infinite-range correlation [20, 42]. Unlike the short-range  $C_1$  term whose spatial variation is multiplicative in displacement of the source and detector, and the  $C_2$  term which is additive in this regard, the  $C_3$  term is independent of displacement of either the source or detector. The cumulant intensity correlation function is given by  $C = C_1 + C_2 + C_3$ . Higher order terms involving odd numbers of Hikami boxes have the spatial dependence of  $C_2$ , whereas terms involving even numbers of Hikami boxes have no spatial variation.

### 3. SIGNATURES OF LOCALIZATION

A sharp divide exists in the nature of wave propagation [61]. On one side, average transport is not appreciably influenced by wave interference. The wave moves a distance,  $\ell \gg \lambda$ , before being randomized in direction and, on scales much larger than  $\ell$ , the intensity or charge density follows a diffusion equation. This leads to a transmission coefficient,  $T_a \sim \ell/L$ , on length scales shorter than the diffusive absorption length,  $L_a = \sqrt{D\tau_a}$  [7], where  $D = \frac{1}{3}v_E\ell$  is the diffusion coefficient,  $v_E$  is the energy transport velocity [62, 63], and  $\tau_a$  is the absorption time. For  $L > L_a$ , the wave is attenuated exponentially. The scale dependence of transmission through a wedge-shaped sample of random titania particles dispersed in polystyrene is shown in Fig. 1.7 [7]. The curve gives the fit of the envelope of the data to diffusion theory. The correlation function of intensity with frequency shift measured in the far field is found to coincide with the square of the Fourier transform of the measured time-of-flight distribution [8]. Hence it corresponds to the  $C_1$  contribution to  $C$ . For diffusive waves, the degree of intensity or current correlation is small, and so  $\text{var}(s_{ab}) \sim 1$ , and  $\text{var}(s_a) \ll 1$ .

On the other side of the divide, the constructive interference of waves returning to a point leads to a suppression of transport. The enhancement of intensity in the backscattered direction in a cone of angular width  $1/k\ell$ , where  $k$  is the wave number, may be viewed as a precursor to localization [64, 65, 66, 67]. The coherent backscattered cone is the Fourier transform of the point spread function on the input surface. Thus it broadens as the wave is more strongly confined. Such backscattering evidently becomes large when  $k\ell \sim 1$ . The

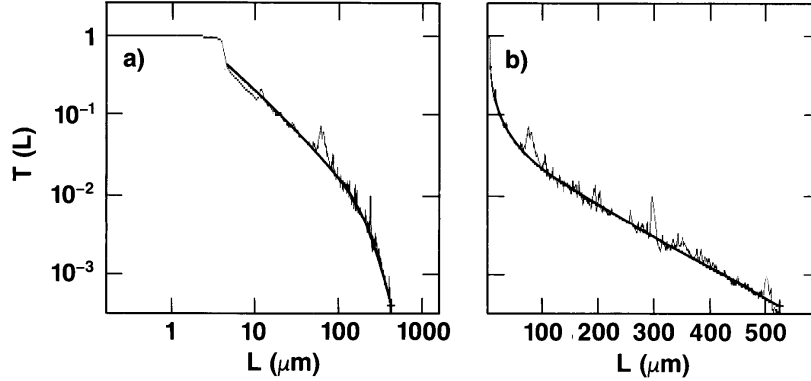


Figure 1.7 (a) Log-log and (b) semilog plots of normalized optical transmission through a wedge of rutile titania powder in a polystyrene matrix. The plots show the inverse and exponential attenuation of transmission with  $L$  for  $L$  smaller than and greater than  $L_a$ , respectively.

wave then cannot be envisioned as propagating with well defined wavelength between scattering centers, and the particle diffusion picture breaks down [68].

Localization by disorder was first discussed in the electronic context. Anderson showed that electrons on an atomic lattice with disorder in the site energy become localized when this disorder exceeds the off-diagonal coupling between neighboring sites [55]. The wave functions then fall exponentially in space, and transport is absent in unbounded samples. In bounded samples, however, electrons may flow through the sample as a result of exponential coupling to the boundary. The Ioffe-Regel criterion [68] for the breakdown of diffusive, particle-like propagation,  $k\ell \sim 1$ , suggests the wave origin of the localization transition. This was further elaborated by John *et al.* [58, 59], who argued that classical waves as well as quantum mechanical waves could be localized.

Edwards and Thouless [56] argued that electrons would be localized when electron states in a block of material could not be shifted into resonance with a neighboring block as a result of interactions at the sample boundary. One measure of the coupling at the boundary is the level width induced by the coupling of the wave to the boundary,  $\delta E$ . Equivalently, the level width may be expressed in frequency units as  $\delta\nu = \delta E/h$ . The level width  $\delta\nu$  may be identified with the inverse of the particle dwell time within the sample block. It may also be quite naturally defined as the correlation frequency, which is the width of the field correlation function with frequency shift. When  $\delta\nu$  falls below the frequency spacing between the levels in equivalent blocks,  $\Delta\nu$ , which is the inverse of the density of states in the block, the coupling between adjacent blocks of material is inhibited. The lines associated with consecutive levels in two blocks of material that may be brought together are shown schematically

in Fig. 1.8. Abrahams *et al.* [57] reasoned that when the dimensionless ratio,

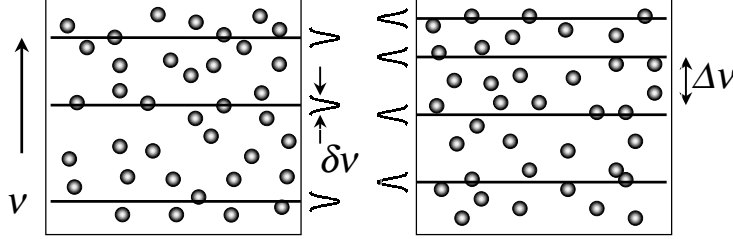


Figure 1.8 Schematic representation of the (mis)matching of modes in two adjacent blocks of a random medium. Here the level width  $\delta\nu$  is smaller than the typical level spacing  $\Delta\nu$ .

$\delta = \delta\nu/\Delta\nu$ , is below unity, this quantity will fall exponentially as the sample is scaled up in size [57]. Using the Einstein relation,  $\sigma = e^2 D(dn/dE)$ , where  $\sigma$  is the conductivity,  $D$  is the diffusion coefficient, and  $dn/dE$  is the density of states per unit volume, it can be shown that  $g = \sigma A/L = \delta$  [57]. Since the scaling of  $g = \delta$  depends upon nothing but the degree of overlap of levels in adjacent blocks of material, which is given by  $\delta$ , it was argued that  $g$  is a universal scaling parameter whose scaling depends only upon the value of  $g$  [57]. For localized waves, average transmission quantities scale exponentially. Because fluctuations in conductance may be significant, especially for localized waves, scaling relations cannot refer to the value of  $g$  for some particular sample realization. Rather they must relate to the ensemble average value of  $g$ .

In contrast to the exponential scaling of  $g$  for localized waves, the conductance scales as  $A/L$  in conducting samples. Both  $g$  and  $\delta$  increase with this scaling factor, as the sample size increases proportionately in three dimensions. Thus  $g$  increases as all dimensions are increased for conducting samples and falls for localized samples. The threshold for localization in three dimensions occurs at the fixed point for the scaling of conductance, at which point the level width remains equal the level spacing,  $\delta = g = 1$ , as the sample size increases. The corresponding transmission for a cube at the localization threshold scales as  $T_a = g/N \sim 1/(kL)^2 \sim (\ell/L)^2$  [57].

>From the foregoing, it is clear that the nature of transport in electronic samples is reflected in the scaling of conductance. The scaling of conductance, at the localization threshold and for localized waves, requires that the wave function be coherent throughout the sample. However, the  $A/L$  scaling of conductance holds in conducting samples, even in the presence of inelastic scattering. The situation is less clear cut, however, for classical waves because the number of particles associated with the field is not conserved [59, 69, 70, 71,

72, 76]. The particle number may be reduced by absorption or augmented by gain. We have seen that in the presence of absorption, for example, transmission falls exponentially for  $L > L_a$ . Thus exponential decay of transmission is not an unambiguous sign of localization.

An example of transmission of a classical wave in a strongly scattering sample is shown in Fig. 1.9 [73, 74]. The figure gives the scale dependence of

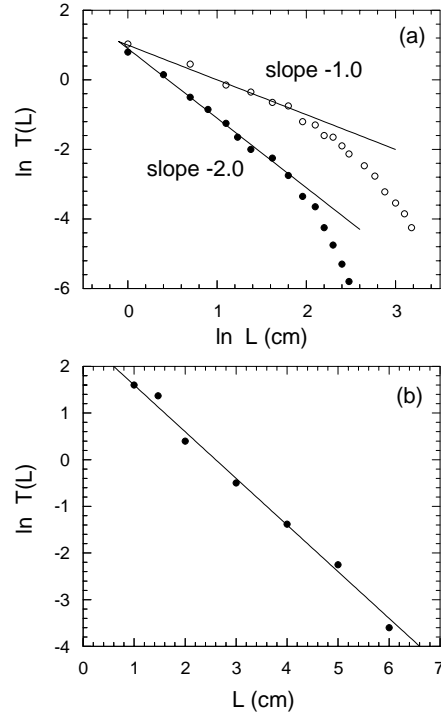


*Figure 1.9* Scale dependence of relative transmission for three volume fractions  $f$  of aluminum in mixture with Teflon spheres: (a) in samples with  $f = 0.20$  (circles), transmission falls inversely with  $L$ , whereas it falls inversely with  $L^2$  in samples with  $f = 0.30$  (filled circles); (b) in samples with  $f = 0.35$ , transmission falls exponentially. The variation of the scaling of transmission is the same as that expected for a transition from diffusive to critical to localized waves in the absence of absorption.

microwave transmission in mixtures of aluminum and Teflon spheres with diameters of 0.47 cm at 19 GHz. At an aluminum sphere volume filling fractions of  $f = 0.20$ , transmission decays inversely with length, from  $L = 1$  cm to  $L = 7$  cm, indicating diffusive transport. At  $f = 0.30$ , transmission falls inversely with  $L^2$ , suggesting that the localization threshold is reached. An accurate absolute determination of transmission was not made, but  $g$  was of

the order of unity in this sample for  $L < 7$  cm. At a higher concentration of  $f = 0.35$ , transmission falls exponentially suggesting the wave is localized. But the possibility that absorption influences transport could not be ruled out.

In more recent experiments, Wiersma *et al.* [75] found a transition from  $1/L$  to  $1/L^2$  to exponential in the thickness dependence of infrared transmission in a wedge of GaAs particles, as the size of particles was changed. The wavelength was in the band gap of GaAs and low absorption was expected. A broadening of the coherent backscattering peak indicated a small value for the transport mean free path. The possibility that these measurements were influenced by absorption has been raised [76]. One interesting feature of the measurements is that the value of  $g$  for a cubic region of the sample with sides equal to the sample thickness  $L$  is significantly larger than unity. This is seen by multiplying the number of modes in an area  $L^2$  by the measured transmission coefficient.

Exponential decay in optical transmission in a sample with low absorption has also been observed recently by Vlasov *et al.* [77] in a nearly periodic opal structure. Again, the value of  $g$  was much larger than unity for cubic regions of the sample for small values of  $L$ . The exponential fall-off of transmission may be related to the evanescent nature of the wave in the nearly periodic structure.

Because of the existence of a variety of explanations for the observations of exponential decay in transmission of electromagnetic radiation, there has not been a consensus on the interpretation of these experiments. The scaling of the average transmission taken by itself is not an unambiguous indication of localization. Furthermore, even in the absence of absorption, the issue of the extent to which the value of the conductance, or equivalently the Lyapunov exponent,  $\gamma = -\langle \ln(g)/L \rangle$ , can give the magnitude of relative fluctuations in conductance arises [78, 79]. In single parameter scaling theory, the magnitude of fluctuations is given in terms of average conductance via the relation,  $\text{var}(\ln(g)/L) = -2\gamma/L$ . But this relation can be violated, as is found in one-dimensional random systems when the typical distance between localization centers is smaller than the localization lengths of these states, allowing their wave functions to overlap [80, 81].

We have seen that an important aspect of transport, which is not present for electrons, is absorption of the wave. The role of absorption is quite different from dephasing of electrons, since absorption does not lead to a reduction of interference of backscattered waves but simply reduces the amplitude of these waves. Weaver [69] showed in simulations of acoustic waves on a two-dimensional lattice that a localized acoustic excitation remains localized in space when dissipation is introduced. The impact upon localization of absorption is not accurately represented by its affect on the conductance. Absorption suppresses transmission and hence transmittance or conductance, at the same time it weakens the affect of localization. But a reduction of conductance is ordinarily seen as a sign of the strengthening of localization. We therefore

seek an indicator of localization, which accurately gives the proximity to the localization threshold in samples both with and without absorption. Similarly, the presence of gain may change the relation between average transport and fluctuations, and an appropriate localization parameter is required in this case.

We also note that, in the presence of absorption,  $g$  and  $\delta$  are affected differently. Whereas  $g$  falls,  $\delta$  increases since the lines broaden due to absorption. Thus these parameters do not reflect the state of transport in the same way. Though we expect that an additional parameter is added when absorption or gain are present, we still seek a parameter that indicates the extent of localization affects.

#### 4. STATISTICS OF DIFFUSIVE WAVES

The first measurements of the distribution of total transmission were carried out by De Boer *et al.* [32] in optical studies in slabs of titania particles. Samples with  $g > 10^3$  were studied and the distribution was found to be a Gaussian to within 1%. A measure of the deviation of the distribution from a Gaussian is the value of the third cumulant  $\langle s_a^3 \rangle_c$ , which gives the skewness of the distribution and vanishes for a Gaussian distribution. For the samples studied,  $\langle s_a^3 \rangle_c$  was of order  $10^{-6}$ .

Greater deviations were observed by Stoytchev and Genack [38] in measurements of the probability distribution of total transmission of microwave radiation in quasi-one-dimensional random waveguides. The samples consisted of 1.27-cm-diam. polystyrene spheres randomly positioned in a copper tube at a volume filling fraction  $f = 0.55$ . Spectra of total transmission over the frequency range 16.8-17.8 GHz were taken at tube diameters of 7.5 and 5.0 cm and at various sample lengths using an integrating sphere. The distributions of normalized total transmission,  $P(s_a)$ , for three ensembles of samples with different external dimensions are shown in Fig. 1.10. In the absence of absorption, the dimensionless conductance,  $g = N\ell/L$ , would be approximately 15.0, 9.0, and 2.25 for samples  $a$ ,  $b$ , and  $c$ , respectively. The distributions are markedly non-Gaussian, and the deviations from Gaussian become more pronounced as either the sample length increases or the tube diameter decreases. A value of  $\langle s_a^3 \rangle_c$  as large as  $0.112 \pm 0.003$  was found for sample  $c$ . Deviations from Gaussian in the tail of the distributions can be seen in the semi-logarithmic plot in Fig. 1.10b. For large  $s_a$ , the distribution has an exponential tail.

Since the distributions of intensity and of total transmission are affected by absorption,  $P(s_a)$  cannot be simply related to  $g$ . But, it was found in these strongly absorbing samples that the distribution  $P(s_a)$  can be well expressed in terms of a single parameter,  $var(s_a)$ , or equivalently  $g' = 2/3var(s_a)$ . In the absence of absorption in the limit  $g \gg 1$ , the full transmission distribution

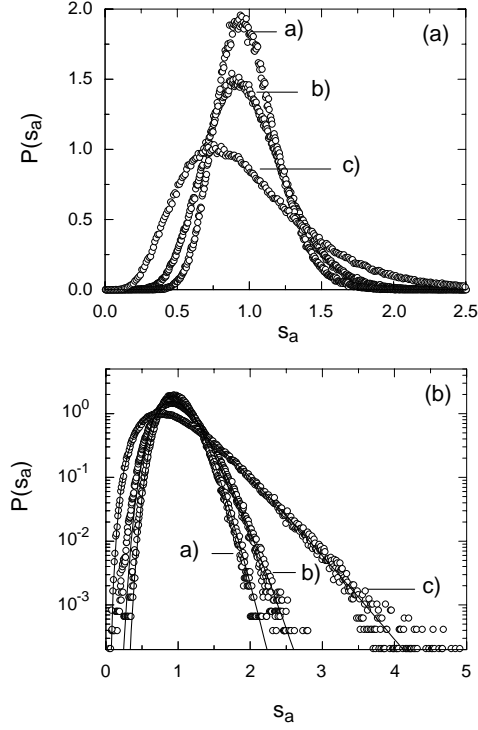


Figure 1.10 Linear (a) and semi-logarithmic (b) plot of the distribution function of the normalized transmission  $P(s_a)$  for three samples with dimensions: a),  $d = 7.5$  cm,  $L = 66.7$  cm; b),  $d = 5.0$  cm,  $L = 50$  cm; c),  $d = 5$  cm,  $L = 200$  cm. Solid lines in (b) represent theoretical results obtained from Eq. (1.3), with measured values of  $g'$  substituted for  $g$  in (1.4).

is given by

$$P(s_a) = \int_{-i\infty}^{i\infty} \frac{dx}{2\pi i} \exp(xs_a - \Phi(x)), \quad (1.3)$$

where

$$\Phi(x) = g \ln^2(\sqrt{1 + x/g} + \sqrt{x/g}) \quad (1.4)$$

is the generating function [33, 34]. It follows from Eqs. (1.3) and (1.4), that  $\text{var}(s_a) = 2/3g$ , and hence  $P(s_a)$  can be expressed in terms of  $\text{var}(s_a)$ . Plots of  $P(s_a)$  of (1.3), obtained after substituting measured values of  $\text{var}(s_a)$  into (1.4), are shown as the solid lines in Fig. 1.10b. They are in excellent agreement with the measured transmission distributions. This suggests that  $\text{var}(s_a)$  is the essential parameter describing transmission fluctuations in random media, even in the presence of absorption. Since the distribution  $P(s_{ab})$  of the normalized

intensity is given by the transform (1.1),  $var(s_a)$  is characteristic for statistics of transmitted intensity as well.

The assumptions underlying Rayleigh statistics for transmitted intensity in non-absorbing samples can be expressed by the condition,  $g \gg 1$ . Deviations in the tail of the distribution  $P(s_{ab})$  were observed in microwave experiments in samples with  $g \approx 10$  [23, 29] and related to the degree of spatial intensity correlation. Corrections to the Rayleigh distribution were calculated by Nieuwenhuizen and van Rossum [33] and by Kogan and Kaveh [34]. They found that the distribution has a stretched exponential tail,  $P(s_{ab}) \sim \exp(-2\sqrt{gs_{ab}})$ , for  $s_{ab} \gg g = \xi/L$ . Similar behavior, but with  $g'$  substituted for  $g$ , was found in strongly absorbing samples. Measurements of the intensity distribution of microwave radiation in random waveguides with lengths up to  $L$  equal to the localization length in the quasi-one-dimensional tube,  $\xi = N\ell$ , were reported in [41]. Samples of loosely packed, 1.27-cm-diam. polystyrene spheres with a filling fraction  $f = 0.52$  were studied within the frequency range 16.8-17.8 GHz. In these samples,  $\ell \approx 5$  cm [82], giving  $\xi \approx 5$  m for a tube diameter of 5 cm. The exponential attenuation length due to absorption is  $L_a = 0.34 \pm 0.02$  m [38], and the diffusion extrapolation length, which gives an effective sample length for the statistics of transmission [83],  $\tilde{L} = L + 2z_b$ , is  $z_b \approx 6$  cm [82]. The distributions measured in three different ensembles of samples are presented in the semi-logarithmic plot in Fig. 1.11. For sample  $a$ , in which

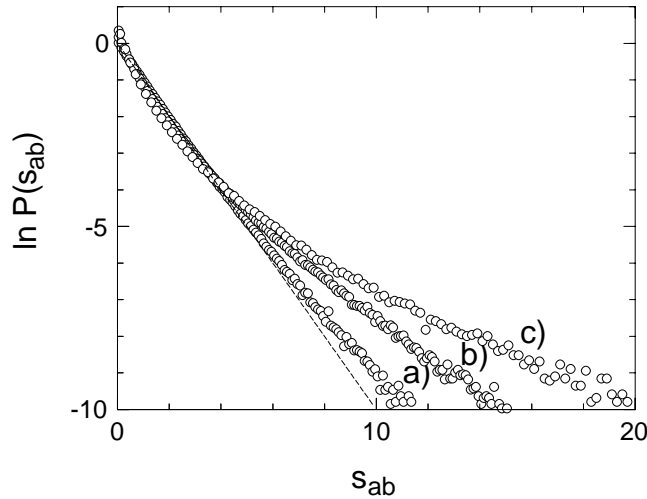
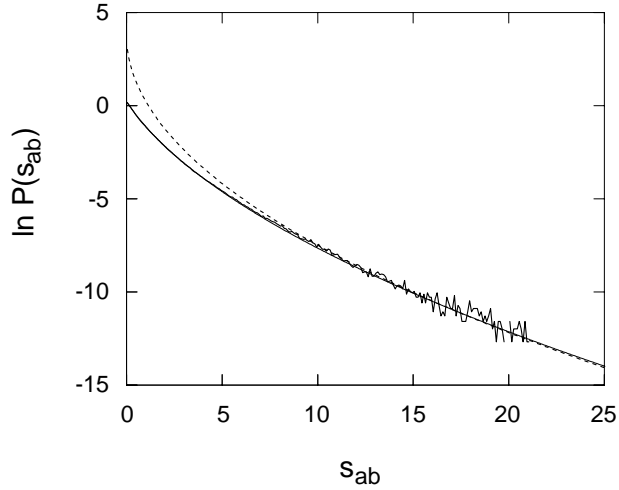


Figure 1.11 Normalized intensity distribution  $P(s_{ab})$  for three samples of dimensions:  $a)$ ,  $d = 7.5$  cm,  $L = 66.7$  cm;  $b)$ ,  $d = 5.0$  cm,  $L = 200$  cm;  $c)$ ,  $d = 5.0$  cm,  $L = 520$  cm. The Rayleigh distribution is shown as the short-dashed line.

$L/\xi = 1/15$ , the distribution is close to a negative exponential. But, as  $L/\xi$  increases, deviations from Rayleigh statistics increase. To study the tail of the normalized intensity distribution  $P(s_{ab})$  for  $s_{ab} \gg \xi/L$ , the measured distributions were fit to the theoretical expression, using  $g'$  as a free parameter. The result of the fit for sample  $b$  is presented as a dotted line in Fig. 1.12. For samples, for which  $P(s_a)$  was also measured, the values of the fitting parameter  $g'$  were found to be within 10% of the values of  $g' = 2/3\text{var}(s_a)$ . The intensity distribution was also compared to the transform (1.1) of the measured transmission distribution. The transform for sample  $b$  is shown as a smooth solid line in Fig. 1.12, which essentially overlaps with the measured distribution. These measurements, therefore, confirm that  $P(s_{ab})$  has a stretched exponen-



*Figure 1.12* Comparison of experimental and theoretical results obtained for sample  $b$ . The smooth solid curve represents the transform (1.1) of the measured total transmission distribution  $b$ ) of Fig. 1.10. The short-dashed line gives the fit to the tail with the theoretical result,  $P(s_{ab}) \sim \exp(-2\sqrt{g's_{ab}})$ . The value of the fitting parameter,  $g' = 3.20$ , is close to the value,  $g' = 3.06$ , obtained from the total transmission measurement for the same sample.

tial tail to the power of  $1/2$  and is given by the transform (1.1) of  $P(s_a)$ . Since  $\text{var}(s_a) = 2/3g$  for  $L \ll \xi$ ,  $L_a$ , and because the localization threshold occurs at  $g = 1$  in the absence of absorption, we make the conjecture that localization is achieved when  $g' = 1$ , or equivalently when  $\text{var}(s_a) = 2/3$ , whether absorption is present or not.

In strongly absorbing quasi-one-dimensional dielectric samples,  $\text{var}(s_a)$  was found to increase sublinearly with length for diffusive waves [38]. This raised the possibility that the value of  $\text{var}(s_a)$  might saturate with length and

that absorption might introduce a cutoff length for the growth of relative fluctuations. Here we show that, though the presence of absorption leads to a decrease in  $\text{var}(s_a)$ , this appropriately reflects a lessening of localization effects. The threshold for localization occurs at  $g' = 1$ , and for smaller values,  $g'$  falls exponentially with length.

We now consider the scaling of  $\text{var}(s_a)$  in the polystyrene samples and its connection to localization. The role of absorption is investigated by comparing measurements to an analysis of the data that statistically eliminates the influence of absorption. For  $L \ll \xi$ ,  $L_a$ , diffusion theory gives  $\text{var}(s_a) = 2\tilde{L}/3\xi$  [33, 34]. This result is shown as the horizontal short-dashed line in Fig. 1.13. As  $g \rightarrow$

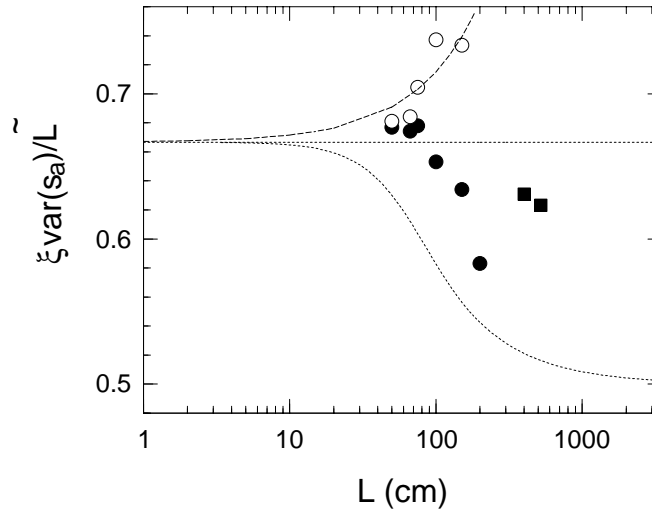


*Figure 1.13* Influence of absorption and localization, separately and together, on  $\text{var}(s_a)$  in random polystyrene samples. A semi-logarithmic plot of  $\xi \text{var}(s_a)/\tilde{L}$  is presented to illustrate the measured scaling of  $\text{var}(s_a)$  over a large range of  $L$ , as well as various theoretical predictions. The upper and lower short-dashed lines represent the two limits of diffusion theory:  $L \ll \xi$ ,  $L_a$  and  $L_a \ll L \ll \xi$ , respectively. The filled circles are obtained from measurements of total transmission, while the filled squares are obtained from measurements of intensity. The circles are the results of an analysis that eliminates the affect of absorption, as explained in the text. The upper, long-dashed curve is a fit of these results to an expression incorporating the first-order localization correction to diffusion theory.

1 and localization threshold is approached, the scaling theory of localization suggests that  $g$  falls more rapidly [57], and hence  $\text{var}(s_a)$  should increase superlinearly with sample length. Measurements of fluctuations in spectra of total transmission in ensembles of polystyrene samples give the results shown as the filled circles in Fig. 1.13. These results indicate that  $\text{var}(s_a)$  increases

sublinearly with length up to  $L = 2$  m, which was the largest length at which accurate measurements of the total transmission could be made.

To extend these studies of statistics in random waveguides to samples of greater lengths, we use Eq. (1.2). This allows us to relate the variance of the normalized total transmission to the variance of the normalized intensity, which is more readily measured in microwave experiments,

$$2\text{var}(s_a) = \text{var}(s_{ab}) - 1. \quad (1.5)$$

Transmitted field spectra are measured in an ensemble of 2,000 polystyrene samples with use of a Hewlett-Packard 8772C network analyzer. The calculated intensity spectra yield  $\text{var}(s_{ab})$  which gives the corresponding values of  $\text{var}(s_a)$  using Eq. (1.5). Values of  $\text{var}(s_a)$  obtained in this way for  $L \leq 2$  m agree within 3% with those shown as the filled circles in Fig. 1.13. The results for  $L > 2$  m are shown in the figure as the filled squares. They indicate a more rapid, superlinear increase in  $\text{var}(s_a)$  relative to the data for  $L \leq 2$  m.

In these measurements, the affect of developing localization and absorption are intertwined. In order to obtain the values of  $\text{var}(s_a)$  that would be measured in the absence of absorption, we use a procedure which is illustrated in Fig. 1.14. The measured field spectra are multiplied by the Fourier transform of a Gaussian pulse in time to give the transmission spectra for this pulse. The spectrum is Fourier transformed to give the temporal response to a short incident Gaussian pulse. To compensate for losses due to absorption, the time dependent field is multiplied by  $\exp(t/2\tau_a)$ , where  $t$  is the time delay from the incident pulse and  $1/\tau_a$  is the absorption rate determined from measurements of the field correlation function with frequency shift [23]. Since the intensity is the square of the field, the decay rate of the field is one half that of the intensity. The intensity of the modified field is shown as the short-dashed line in Fig. 1.14. This modified field is then transformed back to the frequency domain. Intensity spectra and the distribution and variance of intensity are then computed. The intensity distributions are in excellent agreement with calculations for diffusive waves [33, 34], which are described in terms of a single parameter  $g$ . The values of  $\text{var}(s_a)$  found in this way are shown as the circles in Fig. 1.13. A fit of the leading order localization correction [42],  $\text{var}(s_a) = 2\tilde{L}/3\xi + 4\tilde{L}^2/15\xi^2$ , to the data gives the upper long-dashed curve in Fig. 1.13 with  $\xi = 5.51 \pm 0.18$  m and  $z_b = 5.25 \pm 0.31$  cm. The results are consistent with independent determination of these parameters [82]. The difference between the circles and the filled circles represents the amount by which  $\text{var}(s_a)$  is reduced by absorption, and hence represents the extent to which absorption suppresses localization.

For diffusing waves,  $\text{var}(s_a)$  was predicted to fall from  $2\tilde{L}/3\xi$  for  $L \ll L_a$  to  $\tilde{L}/2\xi$  for  $L \gg L_a$  [30, 39], following the lower short-dashed curve in Fig. 1.13. Notwithstanding the initial drop of  $\text{var}(s_a)$  from  $2\tilde{L}/3\xi$ , our measurements rise

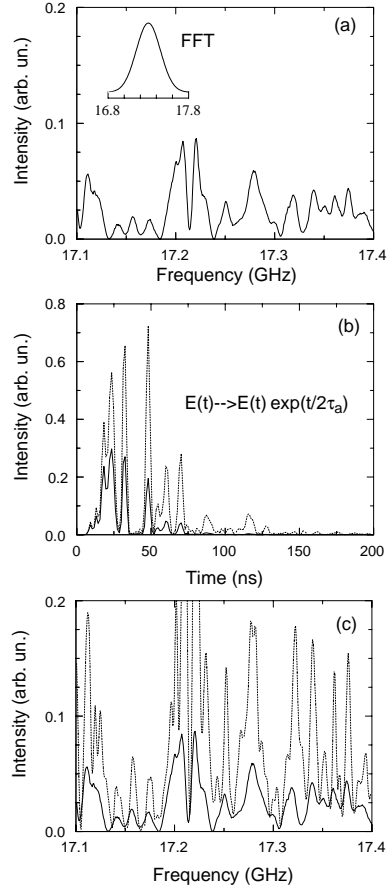


*Figure 1.14* Statistical cancellation of absorption. (a) Intensity spectrum in a sample from the same ensemble as in Fig. 1.2. The field spectrum, from which the intensity spectrum is obtained, is multiplied by the spectrum of the pulse shown in the inset of (a) and Fourier transformed to the time domain. The result of the transform is squared to give the intensity pulse shown in (b) as the solid curve. The influence of absorption is removed in a statistical sense by multiplying field of the pulse by a factor  $\exp(t/2\tau_a)$ . The intensity of the modified pulse is shown as the short-dashed line in (b). The modified field is then Fourier transformed to the frequency domain. The field spectrum is then squared to give the transmitted intensity spectrum shown in (c) as the short-dashed curve and compared to the original spectrum. Intensity statistics computed using the transformed spectra are the same as predicted for a medium with the same real part of the dielectric function but without absorption.

above this curve as a result of enhanced intensity correlation, as  $L \rightarrow \xi$ . At  $L = 5.2$  m,  $\text{var}(s_a) = 0.6$ , which is close to the critical value  $2/3$ .

## 5. STATISTICS OF LOCALIZED WAVES

To study the statistics of transmission quantities for localized waves, we examine fluctuations of intensity in strongly scattering quasi-one-dimensional samples of alumina ( $\text{Al}_2\text{O}_3$ ) spheres (see Fig. 1.15). In order to have control

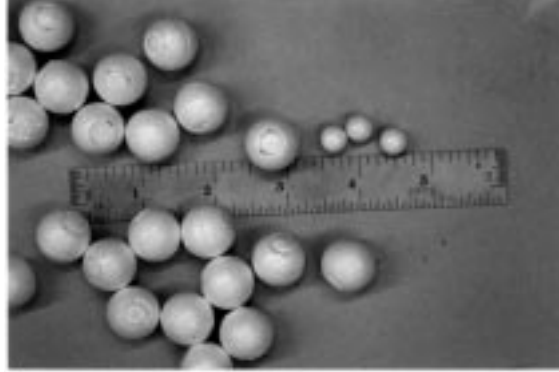


*Figure 1.15* Alumina samples are composed of  $\frac{3}{8}$ -in-diam. alumina ( $\text{Al}_2\text{O}_3$ ) spheres embedded in Styrofoam spheres. Styrofoam is nearly transparent for microwave and serves to control over alumina concentration. In the picture, spheres with diameter of  $\frac{3}{4}$  in. are shown. An inch ruler is also shown.

over the alumina concentration, the alumina spheres (diameter  $d_A = 0.95$  cm, dielectric constant  $\epsilon_A = 9.86$ ) are embedded in Styrofoam spheres of  $\epsilon_S = 1.05$ . The scattering efficiency of the alumina spheres can be inferred from measurements of microwave transmission in optically thin, low concentration ( $f < 0.001$ ) alumina samples. Extinction of the microwave radiation measured in such samples over the frequency range 11.8-19.0 GHz is shown in Fig. 1.16. We also used Mie theory to obtain the scattering efficiency  $Q_{sc}$  for the alumina sphere over the frequency range 7-19 GHz. In calculations, we assumed the alumina sphere to be lossless, and the numerical value of  $\epsilon_A = 9.86$  was adjusted until the positions of the Mie resonances were located under the dips in the experimental data in Fig. 1.16.

We measure microwave field transmitted through an ensemble of alumina scatterers randomly positioned in a 7.3-cm-diam. copper tube at an alumina volume fraction  $f = 0.068$ . Large values of  $var(s_a)$  indicate that the wave is localized near the first Mie resonance of the alumina sphere. A typical spectrum of  $s_{ab}$  obtained in the localization region is shown in Fig. 1.17. The sharp peaks in  $s_{ab}$  appear to be related to resonant transmission through localized photonic states in the sample. We expect that when the frequency of the incident wave is tuned to resonance with localized states in the medium, transmission is appreciable. Between the peaks, transmission is exponentially small and the incident

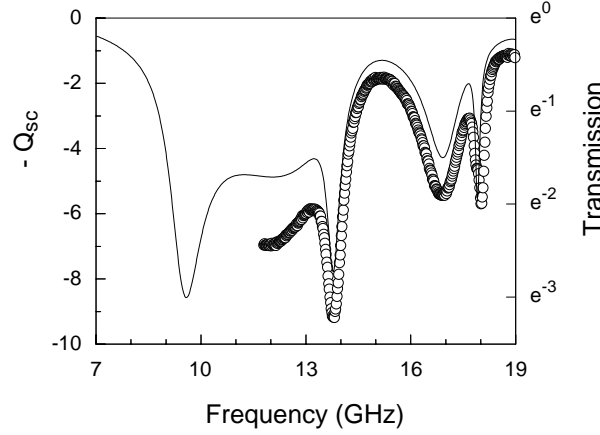


*Figure 1.16* Measured transmission of the microwave radiation in an optically thin, low concentration ( $f < 0.001$ ) alumina sample is shown over the frequency range 11.8-19.0 GHz. Plotted on semi-logarithmic scale, extinction of microwave radiation indicates frequency dependence of scattering efficiency of the alumina sphere. The scattering efficiency  $Q_{sc}$  for the alumina sphere was obtained from Mie theory, and the negative of  $Q_{sc}$  is shown as the solid curve over the frequency range 7-19 GHz.

wave is almost completely reflected from the medium. The distribution function  $P(s_{ab})$  calculated for an ensemble of 5,000 samples is shown in Fig. 1.18 and compared to the Rayleigh distribution. The measured distribution is remarkably broad with  $var(s_{ab}) = 23.5$ , and fluctuations greater than 300 times the average value are observed. The scaling of  $var(s_a)$  determined using Eq. (1.5) at a number of frequencies near the first resonance is shown in Fig. 1.19. We find that  $var(s_a)$  increases exponentially once it becomes of order unity, as expected for a localization parameter.

The availability of a measurable localization parameter makes it possible to determine the existence and the extent of localization in a variety of samples. This is illustrated in measurements of localization in periodic metallic wire meshes containing metallic scatterers. John [85] has proposed that photon localization could be achieved by introducing disorder in a periodic structure possessing a photonic band gap. These band gaps exist in the electromagnetic spectrum of a variety of periodic structures in analogy with the electronic band gaps in crystals [86]. In the photonic band gap, electromagnetic waves are evanescent. When disorder is introduced in such structures, localized states are created in the gap. The periodic structure that we examine is a simple cubic lattice made up of copper wires, with a lattice constant of 1 cm. The lattice has eight unit cells along each side and is enclosed in a section of a

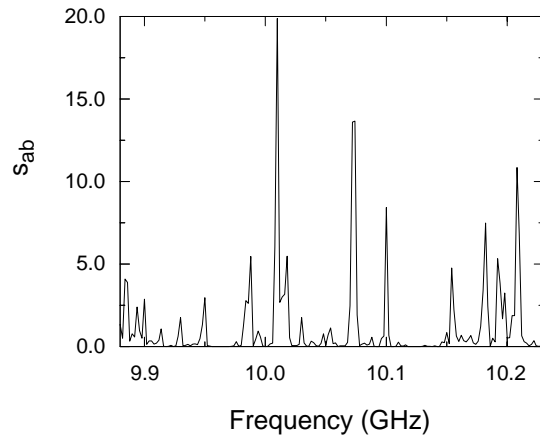


*Figure 1.17* A typical spectrum of the normalized intensity  $s_{ab}$  near the first Mie resonance of the alumina spheres in a 80-cm-long alumina sample. The sharp and narrow line spectra and giant fluctuations shown have been predicted for localized waves and are unlike the corresponding spectrum in diffusive sample shown in Fig. 1.2.

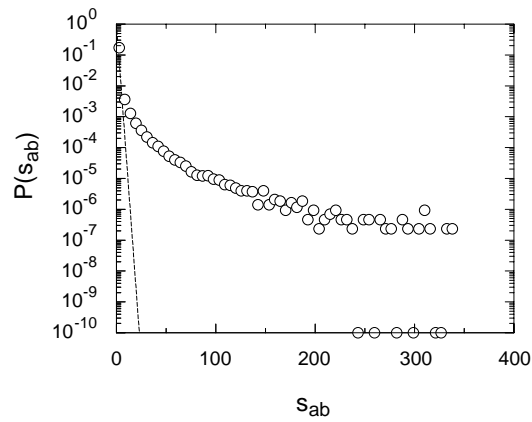


*Figure 1.18* Semi-logarithmic plot of the distribution  $P(s_{ab})$  for the alumina sample. The distribution is obtained in an ensemble of 5,000 spectra within the frequency range 9.88-10.24 GHz, in which statistical parameters do not change substantially. The circle on the horizontal axis represents bins in which there was no measured intensity value. The broken line represents the Rayleigh distribution.

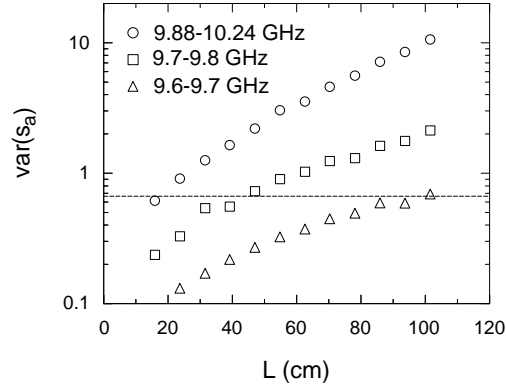
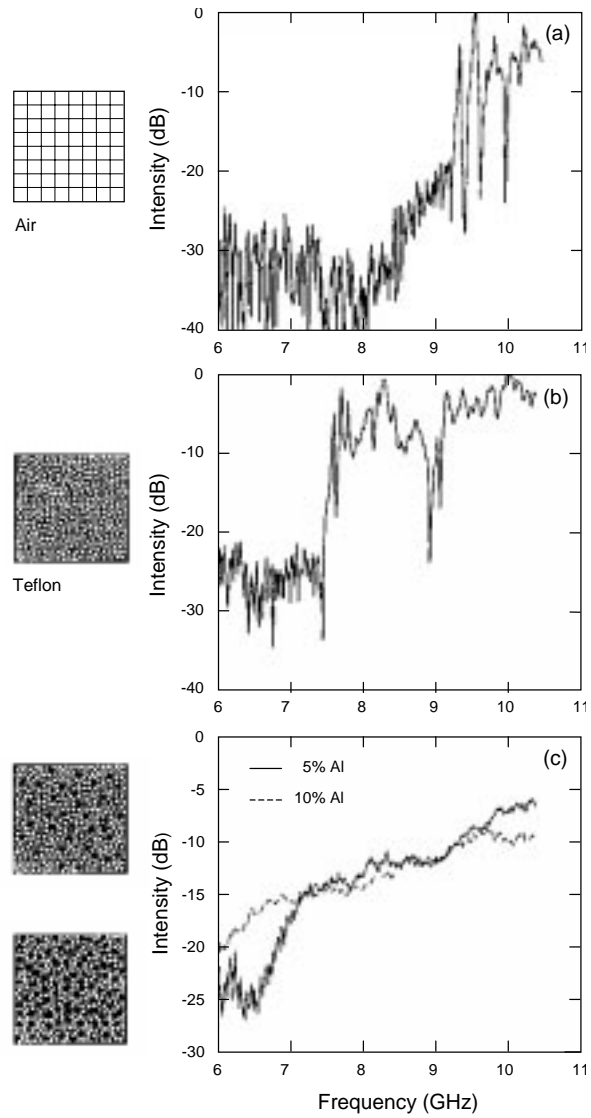


Figure 1.19 Scaling of  $\text{var}(s_a)$  in alumina samples. The values of  $\text{var}(s_a)$  averaged over the indicated frequency intervals are obtained using Eq. (1.5). Above a value of order unity,  $\text{var}(s_a)$  increases exponentially. In the interval 9.88-10.24 GHz,  $\text{var}(s_a) \sim \exp(L/L_{exp})$ , with  $L_{exp} \approx 42$  cm.

square waveguide. Measurements of microwave transmission in an empty wire mesh sample show a low-frequency gap with a cut-off frequency of 9.33 GHz (Fig. 1.20a) [87]. The network is filled with 0.47-cm-diam. Teflon spheres in order to float various scatterers within the structure. The mean free path of randomly positioned Teflon spheres greatly exceeds the length of the structure, so that their only influence is to reduce the wavelength of radiation within the structure. The cut-off frequency shifts to 7.58 GHz (Fig. 1.20b). This is the same fractional shift as the ratio of the wavelength in air to that in a random sample of Teflon spheres, as determined by a measurement of the coherent field transmitted through the sample. Thus the ratio of the cut-off wavelength to the length of the unit cell is a constant in the structure. When aluminum spheres with the same diameter replace some of the Teflon spheres, transmission peaks appear in the gap just below the band edge. As the scatterer density is increased, the gap fills in. Spectra of the average transmission measured in ensembles of 200 sample configurations at two aluminum sphere volume fractions,  $f = 0.05$  and  $f = 0.10$ , are shown in Fig. 1.20c. But such measurements leave open the question of whether the radiation is localized. To answer this question, we compute  $\text{var}(s_a)$  for the two concentrations of aluminum spheres shown in Fig. 1.21. At  $f = 0.05$ , a window of localization is found, in which  $\text{var}(s_a) \geq 2/3$ . At twice this aluminum fraction, the reduced values of  $\text{var}(s_a)$  indicate that wave propagation is diffusive. At this higher concentration, the density of



*Figure 1.20* Schematic diagram of the wire mesh lattice filled with different media and associated transmission spectra. The structure has a lattice constant of 1 cm and is 8 unit cells on each side. In (a), the structure is in air. In (b), it is filled with Teflon spheres. In (c), the structure is filled with Teflon-aluminum mixtures at filling fractions of aluminum spheres of  $f = 0.05$  and  $f = 0.10$ . The average transmission spectra obtained from 200 configurations for each value of  $f$  are shown.

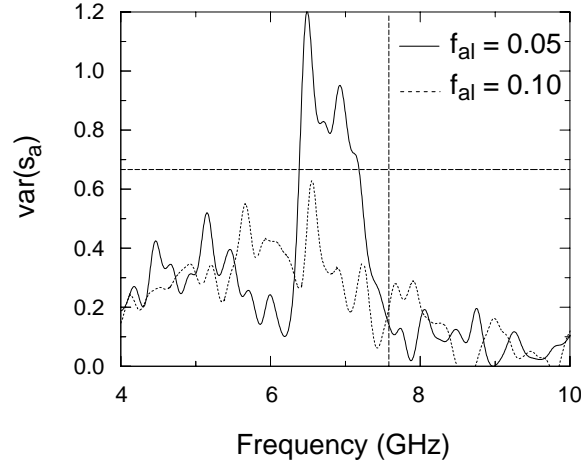


Figure 1.21  $Var(s_a)$  vs. frequency in a metallic wire mesh containing aluminum scatterers. The broken vertical line indicates the position of the band edge in a periodic structure filled only with Teflon spheres. At an aluminum sphere volume fraction  $f = 0.05$ ,  $var(s_a)$  is markedly higher near the edge, rising above the localization threshold of  $2/3$  shown as the broken horizontal line. At  $f = 0.10$ ,  $var(s_a)$  is reduced and wave propagation is diffusive.

states introduced by disorder becomes high enough that the wave is no longer localized. The gap is effectively washed out.

We have also used measurements of  $var(s_a)$  to examine the claim that localization can be achieved in three-dimensional samples of metal spheres at various concentrations [73, 74, 88, 89]. We find that in samples of 0.47-cm-diam. aluminum spheres of length  $L = 8.2$  cm and diameter  $d = 7.5$  cm, with various volume fraction from 0.1 to 0.475,  $var(s_a)$  never rises above the localization threshold of  $2/3$ . A maximum value of 0.29 is reached at  $f = 0.45$ . Thus we conclude that *three-dimensional* localization is not achieved in these aluminum samples.

## 6. SUMMARY

In conclusion, we have demonstrated that the variance of the normalized transmission is a robust localization parameter. It serves as a powerful tool in the search for and characterization of photon localization, even for absorbing samples. It has allowed us to locate regimes of localization in quasi-one-dimensional dielectric samples and in periodic metallic wire lattices containing metallic scatterers, and to rule it out in collections of aluminum spheres. These results show that the statistics of transmission are essential aspects of localization.

## Acknowledgments

We would like to thank Patrick Sebbah for suggesting the topic and title of this presentation and for stimulating discussions and contributions. We are grateful to Piet Brouwer, Eugene Kogan, Victor Kopp, Edward Kuhner, Alexander Lisyansky, Zdzislaw Ozimkowski, Mark van Rossum, Marin Stoytchev, and Bart van Tiggelen for stimulating discussions and technical assistance without which this work would not have been possible. This research was supported by the National Science Foundation under grants DMR-9973959 and INT-9512975 and by a PSC-CUNY award.

## References

- [1] A. Ishimaru, *Wave Propagation and Scattering in Random Media* (Academic Press, New York, 1978).
- [2] J. W. Goodman, *Statistical Optics* (Wiley, New York, 1985).
- [3] *Scattering and Localization of Classical Waves in Random Media*, edited by P. Sheng (World Scientific Press, Singapore, 1990).
- [4] *Mesosopic Phenomena in Solids*, edited by B. L. Altshuler, P. A. Lee, and R. A. Webb (Elsevier, Amsterdam, 1991).
- [5] *Diffuse Waves in Complex Media*, edited by J.-P. Fouque (Kluwer Academic Publishers, Dordrecht, 1999).
- [6] I. Freund and D. Elyahu, Phys. Rev. **A 45**, 6133 (1992).
- [7] A. Z. Genack, Phys. Rev. Lett. **58**, 2043 (1987).
- [8] A. Z. Genack and J. M. Drake, Europhys. Lett. **11**, 331 (1990).
- [9] P. Sebbah, O. Legrand, B. A. van Tiggelen, and A. Z. Genack, Phys. Rev. E **56**, 3619 (1997).
- [10] J. W. Strutt (Lord Rayleigh), Proc. Lond. Math. Soc. **3**, 267 (1871).
- [11] J. C. Dainty, *Laser Speckle and Related Phenomena* (Springer-Verlag, Berlin, 1975).
- [12] R. A. Webb, S. Washburn, C. P. Umbach, and R. B. Laibowitz, Phys. Rev. Lett. **54**, 2696 (1985).
- [13] B. L. Altshuler and D. E. Khmel'nitskii, JETP Lett. **42**, 359 (1985).
- [14] P. A. Lee and A. D. Stone, Phys. Rev. Lett. **55**, 1622 (1985).
- [15] B. Shapiro, Phys. Rev. Lett. **57**, 2168 (1986).
- [16] B. Shapiro, Phil. Mag. B **56**, 1031 (1987).
- [17] M. J. Stephen and G. Cwilich, Phys. Rev. Lett. **59**, 285 (1987).
- [18] G. Maret and P. E. Wolf, Z. Phys. B **65**, 409 (1987).
- [19] P. A. Mello, E. Akkermans, and B. Shapiro, Phys. Rev. Lett. **61**, 459 (1988).

- [20] S. Feng, C. Kane, P. A. Lee, and A. D. Stone, *Phys. Rev. Lett.* **61**, 834 (1988).
- [21] I. Edrei, M. Kaveh, and B. Shapiro, *Phys. Rev. Lett.* **62**, 2120 (1989).
- [22] R. Pnini and B. Shapiro, *Phys. Rev. B* **39**, 6986 (1989).
- [23] N. Garcia and A. Z. Genack, *Phys. Rev. Lett.* **63**, 1678 (1989).
- [24] A. Z. Genack, N. Garcia, and W. Polkosnik, *Phys. Rev. Lett.* **65**, 2129 (1990).
- [25] M. P. van Albada, J. F. de Boer, and A. Lagendijk, *Phys. Rev. Lett.* **64**, 2787 (1990).
- [26] N. Shnerb and M. Kaveh, *Phys. Rev. B* **43**, 1279 (1991).
- [27] E. Kogan and M. Kaveh, *Phys. Rev. B* **45**, 1049 (1992).
- [28] E. Kogan, M. Kaveh, R. Baumgartner, and R. Berkovits, *Phys. Rev. B* **48**, 9404 (1993).
- [29] A. Z. Genack and N. Garcia, *Europhys. Lett.* **21**, 753 (1993).
- [30] N. Garcia, A. Z. Genack, R. Pnini, and B. Shapiro, *Phys. Lett. A* **176**, 458 (1993).
- [31] R. Berkovits and S. Feng, *Phys. Rep.* **238**, 135 (1994).
- [32] J. F. de Boer, M. C. W. van Rossum, M. P. van Albada, Th. M. Nieuwenhuizen, and A. Lagendijk, *Phys. Rev. Lett.* **73**, 2567 (1994).
- [33] M. C. W. van Rossum and Th. M. Nieuwenhuizen, *Phys. Rev. Lett.* **74**, 2674 (1994).
- [34] E. Kogan and M. Kaveh, *Phys. Rev. B* **52**, R3813 (1995).
- [35] V. Fal'ko and K. Efetov, *Phys. Rev. B* **52**, 17413 (1995).
- [36] S. A. van Langen, P. W. Brouwer, and C. W. J. Beenakker, *Phys. Rev. E* **53**, 1344 (1996).
- [37] A. A. Chabanov and A. Z. Genack, *Phys. Rev. E* **56** R1338 (1997).
- [38] M. Stoytchev and A. Z. Genack, *Phys. Rev. Lett.* **79** 309 (1997).
- [39] P. W. Brouwer, *Phys. Rev. B*, **57**, 10526 (1998).
- [40] F. Scheffold and G. Maret, *Phys. Rev. Lett.* **81**, 5800 (1998).
- [41] M. Stoytchev and A. Z. Genack, *Opt. Lett.* **24**, 262 (1999).
- [42] M. C. W. van Rossum and Th. M. Nieuwenhuizen, *Rev. Mod. Phys.* **71**, 313 (1999).
- [43] M. Stoytchev, Ph. D. Thesis (City University of New York, 1998).
- [44] A. A. Chabanov, M. Stoytchev, and A. Z. Genack, *Nature* **404**, 850 (April, 2000).
- [45] R. Pnini in this book.

- [46] P. Sebbah, R. Pnini, and A. Z. Genack, Phys. Rev. E (2000).
- [47] E. Wigner, Phys. Rev. **98**, 145 (1955).
- [48] F. T. Smith, Phys. Rev. **118**, 349 (1960); **119**, 2098 (1960).
- [49] M. Buttiker, H. Thomas, and A. Pretre, Phys. Lett. A **180**, 364 (1993).
- [50] J. G. Muga and D. M. Wardlaw, Phys. Rev. E **51**, 5377 (1995).
- [51] P. W. Brouwer, K. M. Frahm, and C. W. J. Beenakker, Phys. Rev. Lett. **78**, 4737 (1997).
- [52] P. Sebbah, O. Legrand, and A. Z. Genack, Phys. Rev. E **59**, 2406 (1999).
- [53] A. Z. Genack, P. Sebbah, M. Stoytchev, and B. A. van Tiggelen, Phys. Rev. Lett. **82**, 715 (1999).
- [54] B. A. van Tiggelen, P. Sebbah, M. Stoytchev, and A. Z. Genack, Phys. Rev. E **59**, 7166 (1999).
- [55] P. W. Anderson, Phys. Rev. **109**, 1492 (1958).
- [56] J. T. Edwards and D. J. Thouless, J. Phys. **C5**, 807 (1972).
- [57] E. Abrahams, P. W. Anderson, D. C. Licciardello, and T. V. Ramakrishnan, Phys. Rev. Lett. **42**, 673 (1979).
- [58] S. John, H. Sompolinsky, and M. J. Stephen, Phys. Rev. B **27**, 5592 (1983).
- [59] S. John, Phys. Rev. Lett. **53**, 2169 (1984).
- [60] R. Landauer, Phil. Mag. **21**, 863 (1970).
- [61] B. van Tiggelen, in *Diffuse Waves in Complex Media*, edited by J.-P. Fouque (Kluwer Academic Publishers, Dordrecht, 1999).
- [62] M. P. van Albada, B. A. van Tiggelen, A. Lagendijk, and A. Tip, Phys. Rev. Lett. **66**, 3132 (1991).
- [63] A. Lagendijk and B. van Tiggelen, Phys. Rep. **270**, 143 (1996).
- [64] Y. Kuga and A. Ishimaru, J. Opt. Soc. Am. **A1**, 831 (1984).
- [65] M. van Albada and A. Lagendijk, Phys. Rev. Lett. **55**, 2692 (1985).
- [66] P. F. Wolf and G. Maret, Phys. Rev. Lett. **55**, 2696 (1985).
- [67] E. Akkermans, P. E. Wolf, and R. Maynard, Phys. Rev. Lett. **56**, 1471 (1986).
- [68] A. F. Ioffe and A. R. Regel, Prog. Semicond. **4**, 237 (1960).
- [69] R. L. Weaver, Phys. Rev. B **47**, 1077 (1993).
- [70] V. Freilikher, M. Pustilnik, and I. Yurkevich, Phys. Rev. Lett. **73**, 810 (1994).
- [71] M. Yosefin, Europhys. Lett. **25**, 675 (1994).
- [72] J. C. J. Paasschens, T. Sh. Mizirpashaev, and C. W. J. Beenakker, Phys. Rev. B **54**, 11887 (1996).

- [73] N. Garcia and A. Z. Genack, *Phys. Rev. Lett.* **66**, 1850 (1991).
- [74] A. Z. Genack and N. Garcia, *Phys. Rev. Lett.* **66**, 2064 (1991).
- [75] D. S. Wiersma, P. Bartolini, A. Lagendijk, and R. Righini, *Nature*, **390**, 671 (1997); D. S. Wiersma, J. G. Rivas, P. Bartolini, A. Lagendijk, and R. Righini, *Nature* **398**, 207 (1999).
- [76] F. Scheffold, R. Lenke, R. Tweer, and G. Maret, *Nature* **398**, 206 (1999).
- [77] Ya. A. Vlasov, M. A. Kaliteevski, and V. V. Nikolaev, *Phys. Rev. B* **60**, 1555 (1999).
- [78] P. W. Anderson, D. J. Thouless, E. Abrahams, and D. S. Fisher, *Phys. Rev. B* **22**, 3519 (1980).
- [79] P. A. Mello, *J. Math. Phys. (N. Y.)* **27**, 2876 (1986).
- [80] L. I. Deych, D. Zaslavsky, and A. A. Lisyansky, *Phys. Rev. Lett.* **81**, 5390 (1998).
- [81] L. I. Deych, A. A. Lisyansky, and B. L. Altshuler, *Phys. Rev. Lett.* **84**, 2678 (2000).
- [82] N. Garcia, A. Z. Genack, and A. A. Lisyansky, *Phys. Rev. B* **46**, 14475 (1992).
- [83] A. Lagendijk, R. Vreeker, and P. de Vries, *Phys. Lett. A* **136**, 81 (1989).
- [84] A. A. Chabanov and A. Z. Genack, submitted (2000).
- [85] S. John, *Phys. Rev. Lett.* **58**, 2486 (1987).
- [86] J. D. Joannopoulos, R. D. Meade, and J. N. Winn, *Photonic Crystals* (Princeton University Press, Princeton, 1995).
- [87] M. Stoytchev and A. Z. Genack, *Phys. Rev. B* **55**, R8617 (1997).
- [88] K. Arya, Z. B. Su, and J. L. Birman, *Phys. Rev. Lett.* **57**, 2725 (1986).
- [89] C. A. Condat and T. R. Kirkpatrick, *Phys. Rev. Lett.* **58**, 226 (1987).